Regional differences in brain glucose metabolism determined by imaging mass spectrometry

Brief Communication

MOLECULAR METABOLISM

Regional differences in brain glucose metabolism determined by imaging mass spectrometry

André Kleinridders [1,2,3,7], Heather A. Ferris [1,6,7], Michelle L. Reyzer [4,7], Michaela Rath [2,3], Marion Soto [1], M. Lisa Manier [4], Jeffrey Spraggins [4], Zhihong Yang [5], Robert C. Stanton [5], Richard M. Caprioli [4], C. Ronald Kahn [1,*]

ABSTRACT

Objective: Glucose is the major energy substrate of the brain and crucial for normal brain function. In diabetes, the brain is subject to episodes of hypo- and hyperglycemia resulting in acute outcomes ranging from confusion to seizures, while chronic metabolic dysregulation puts patients at increased risk for depression and Alzheimer's disease. In the present study, we aimed to determine how glucose is metabolized in different regions of the brain using imaging mass spectrometry (IMS).

Methods: To examine the relative abundance of glucose and other metabolites in the brain, mouse brain sections were subjected to imaging mass spectrometry at a resolution of 100 μm. This was correlated with immunohistochemistry, qPCR, western blotting and enzyme assays of dissected brain regions to determine the relative contributions of the glycolytic and pentose phosphate pathways to regional glucose metabolism.

Results: In brain, there are significant regional differences in glucose metabolism, with low levels of hexose bisphosphate (a glycolytic intermediate) and high levels of the pentose phosphate pathway (PPP) enzyme glucose-6-phosphate dehydrogenase (G6PD) and PPP metabolite hexose phosphate in thalamus compared to cortex. The ratio of ATP to ADP is significantly higher in white matter tracts, such as corpus callosum, compared to less myelinated areas. While the brain is able to maintain normal ratios of hexose phosphate, hexose bisphosphate, ATP, and ADP during fasting, fasting causes a large increase in cortical and hippocampal lactate.

Conclusion: These data demonstrate the importance of direct measurement of metabolic intermediates to determine regional differences in brain glucose metabolism and illustrate the strength of imaging mass spectrometry for investigating the impact of changing metabolic states on brain function at a regional level with high resolution.

Keywords Brain imaging; Glucose metabolism; Pentose phosphate pathway; Glycolysis; ATP; Mass spectrometry

1. INTRODUCTION

Glucose is the main energy substrate for the brain and accounts for about 20% of whole-body glucose utilization [1–3]. People with diabetes may have periods of hyperglycemia or hypoglycemia, and these changes in glucose can be associated with brain dysfunction ranging from confusion to seizures. In addition, the increased long-term risks of depression and Alzheimer's disease associated with diabetes [4] highlight the importance of insulin action and metabolic status on short- and long-term brain function and survival.

Glucose is metabolized in cells either by glycolysis or the pentose phosphate pathway (PPP). In the glycolytic pathway, glucose is converted to pyruvate which can be converted to lactate by lactate dehydrogenase or sent to the tricarboxylic acid (TCA) cycle to generate ATP via oxidative phosphorylation. Alternatively, glucose can enter the PPP via the action of glucose-6-phosphate dehydrogenase (G6PD) to generate 5-carbon sugars, as well as NADPH, which is a co-factor for cholesterol biosynthesis and protects against oxidative stress [5]. Though each cell can use glucose for either glycolysis or the PPP, different cell populations favor distinct metabolic pathways [6,7].

[1]Department of Integrative Physiology and Metabolism, Joslin Diabetes Center, Harvard Medical School, Boston, MA 02215, USA [2]German Institute of Human Nutrition, Central Regulation of Metabolism, Arthur-Scheunert-Allee 114-116, Potsdam-Rehbruecke, Nuthetal, Germany [3]German Center for Diabetes Research (DZD), Ingolstaedter Land Str. 1, 85764 Neuherberg, Germany [4]Mass Spectrometry Research Center, Vanderbilt University, Nashville, TN 37240, USA [5]Department of Vascular Cell Biology, Joslin Diabetes Center, Harvard Medical School, Boston, MA 02215, USA

[6] Present address: Division of Endocrinology and Metabolism, University of Virginia, Charlottesville, VA 22901, USA.
[7] These authors contributed equally to this work.

*Corresponding author. Joslin Diabetes Center, One Joslin Place, Boston, MA 02215, USA. Fax: +1 (617) 309-2487.

E-mails: andre.kleinridders@dife.de (A. Kleinridders), hf4f@virginia.edu (H.A. Ferris), c.ronald.kahn@joslin.harvard.edu (C.R. Kahn).

Received February 12, 2018 • Revision received March 15, 2018 • Accepted March 24, 2018 • Available online 6 April 2018

https://doi.org/10.1016/j.molmet.2018.03.013

The mouse brain consists of roughly 70% neurons and 30% non-neuronal cells with different brain regions exhibiting distinct compositions of cells [8]. Neurons and astrocytes metabolize glucose mainly via glycolysis for the generation of ATP while oligodendrocytes must generate the cholesterol rich myelin sheaths. Thus, oligodendrocytes shuttle more glucose into the PPP in order to generate NADPH for cholesterol biosynthesis [9]. It has been estimated that 10% of glucose in oligodendrocytes is used for the PPP [10], but this apparently small proportion of glucose may be higher as the PPP seems to be underestimated in comparison to glycolysis by many approaches [11].

To investigate the regional fate of glucose, we assessed multiple steps within the glycolytic and PPP using a combination of gene and protein expression, protein activity assays, and imaging mass spectrometry (IMS). We demonstrate that while measurements of enzyme expression and activity point to differences in the regional activity of glycolysis and the PPP, IMS provides a direct measurement of the metabolites generated in these pathways in specific brain regions, including those which are otherwise difficult to assess, such as the fimbria or corpus callosum. Further, we demonstrate that in these highly myelinated white matter tracts there is a high ATP/ADP ratio but not a similarly high hexose bisphosphate/hexose monophosphate ratio, supporting the notion that the lactate shuttle may be very important for energy metabolism in these brain regions. Thus, IMS provides a powerful tool for high resolution assessment of glucose metabolism across brain regions.

2. MATERIALS AND METHODS

2.1. Animals

All mice were housed in a mouse facility on a 12 h light/dark cycle in a temperature-controlled room. 10–12 week old male C57Bl/6J mice (Jackson Laboratories: stock nr. 000664) were maintained on a standard chow diet (Mouse Diet 9F 5020; PharmaServ). When fasted, animals had free access to water. Animal care and study protocols were approved by the Animal Care Committee of Joslin Diabetes Center and were in accordance with the National Institutes of Health guidelines as well as the animal welfare committees of the German Institute of Human Nutrition (DIfE) and the local authorities (LUGV, Brandenburg, Germany).

2.2. Immunostaining

Mice were anesthetized with an intraperitoneal (i.p.) injection of Avertin (300 mg/kg) and transcardially perfused with PBS followed by 4% paraformaldehyde. Brains were dissected and post-fixed in 4% paraformaldehyde overnight, cryoprotected in 15% (w/v) then 30% sucrose, and frozen in OCT compound (Tissue-Tek). Serial coronal 30 μm sections were washed, blocked (0.2% Triton-X-100 + 5% normal goat serum (NGS) in PBS), and stained with primary antibody (Table A.1) diluted in PBS containing 0.1 Triton X-100 + 1% NGS overnight at 4 °C. Sections were then washed and subsequently stained with secondary antibodies (Vectastain VIP, Vector Labs or goat anti-rabbit Alexa Fluor 488 and goat anti-mouse Alexa Fluor 594, 1:500, ThermoFisher Scientific). Sections were mounted with SlowFade Diamond mountant containing DAPI (Life Technologies) and imaged with a 10× objective on a Zeiss LSM710-Duo confocal microscope.

2.3. Analysis of gene expression by quantitative PCR

Total RNA from brain regions was isolated using an RNeasy Mini Kit (Qiagen). 1 μg of total RNA was reverse transcribed in 20 μl using the High Capacity cDNA Reverse Transcription Kit (Promega). 10 ng of synthesized cDNA was amplified with specific primers in a 10 μl PCR reaction using a SYBR green PCR master mix (Promega). Analysis of gene expression was performed using an ABI ViiA™ 7 Real-Time PCR System with 384-Well Block with initial denaturation at 95 °C for 10 min, followed by 40 PCR cycles, each cycle consisting of 95 °C for 15 s, 60 °C for 1 min, and 72 °C for 1 min, and SYBR green fluorescence emissions were monitored after each cycle. For each gene, mRNA expression was calculated relative to TATA binding protein (TBP) expression. Amplification of specific transcripts was confirmed by the melting-curve profiles.

2.4. Enzyme assays

Phosphofructokinase and hexokinase assays were performed according to manufacturer's guidelines (Sigma), and G6PD activity assay was performed as previously described [12].

2.5. Imaging mass spectrometry and MS/MS

Mice were maintained on a chow diet and sacrificed in random order in the morning after a 16 h overnight fast or following ad libitum access to chow. IMS was performed on five individuals from each treatment group and HP, HBP, ATP, and ADP relative abundance were assessed for regions of interest. Serial sections of the brains were used to analyze lactate.

Gold-coated stainless steel MALDI target plates were precoated with α-cyano-4-hydroxycinnamic acid (CHCA) using an automated sprayer (TM Sprayer, HTX Technologies). CHCA was prepared as 5 mg/ml in 90% acetonitrile and was sprayed at 0.15 ml/min at 100 °C at 700 mm/min plate velocity. Four passes were deposited at 2 mm spacing, alternating horizontal and vertical positions between passes with a 1 mm offset for the second passes in each direction. Sections from fresh frozen mouse brain were obtained at 12 μm thickness in a cryostat. The sections were directly thaw-mounted onto the precoated target plates. The tissues were subsequently post-coated with 9-aminoacridine (9AA) matrix, prepared at 5 mg/ml in 90% methanol, and applied using the same program as for CHCA on the TM Sprayer. Sections designated for lactate imaging were only postcoated with 9AA. Metabolite images were acquired on a 9.4T FT-ICR mass spectrometer (Bruker Solarix, Bruker Daltonics) in negative ionization mode at 100 μm spatial resolution. Tentative metabolite identifications were made based on accurate mass, which is typically better than 2 ppm. Masses were searched against the Human Metabolome Database (www.hmdb.ca) for possible identifications as well as possible isobaric interferences. Because there are numerous structures and linkages possible for hexose phosphate and bisphosphate sugars, we categorize them as generic hexose phosphate and hexose bisphosphate species. Table A.2 shows the likely identifications and ion forms of the metabolites imaged in this work. In order to more fully characterize some species, serial sections were prepared as described above and analyzed for select metabolites via MS^3 imaging on a linear ion trap equipped with a MALDI source and a nitrogen laser (Thermo LTQ XL). Images were acquired at 100 μm spatial resolution with a 50 μm spiral raster for each transition. The following transitions were monitored: ATP: MS^3 m/z 506 → m/z 408 → m/z 273 + 214; ADP: MS^3 m/z 426 → m/z 328 → m/z 134; Glucose-1,6-bisphosphate: MS^3 m/z 339 → m/z 241 → [m/z 79 + 97] + m/z 121 + 139; Fructose-1,6-bisphosphate: MS^3 m/z 339 → m/z 241 → [m/z 79 + 97] + m/z 151. ATP and ADP were imaged together on select sections, and glucose bisphosphate and fructose bisphosphate were imaged together on select sections. These transitions were optimized on standard compounds. The transitions for ATP and ADP are selective enough to distinguish them from exact isomers (dGTP and dGDP). The

dominant fragment ions from the hexose bisphosphates were common to all isomers tested, but some smaller fragment ions were unique to each species, as listed above.

2.6. Experimental design and statistical analysis

Averages across brain regions were compared in control mice. All data are shown as mean values ± standard error of the mean. Comparison of ADP, ATP, HP, and HBP in fed and fasted groups were analyzed for statistical significance using two-way ANOVA with Tukey's post-hoc analysis. For lactate analysis each set of brains were run on a separate plate. Due to variability between runs, the fed brain on each slide was set to 1 and the fasted brain expressed as a percent increase over fed. Brain regions were then compared by paired t-test. All other data sets were analyzed for statistical significance using one-way ANOVA followed by Tukey's post-hoc analysis.

3. RESULTS

3.1. Glucose-6-phosphate dehydrogenase expression correlates with high MBP expression

Different brain regions are composed of different ratios of cell types. Both the activity of a brain region, as well as the cells that compose that region, are likely to influence metabolism in that region of the brain. For glucose metabolism, immunohistochemistry revealed significant differences in the regional distribution of glucose-6-phosphate dehydrogenase (G6PD), the enzyme controlling the rate-limiting step of the pentose phosphate pathway (PPP), with strong staining in the thalamus, intermediate in the motor cortex, and very limited staining in the amygdala/piriform cortex (referred to hereafter as simply amygdala) (Figure 1A,B), consistent with strong regional localization of this enzyme. To address whether this regional difference was due to differences in cellular composition, we estimated the distribution of different cell types in each area by quantitative RT-PCR (qPCR) (Figure 1C) and immunofluorescence (Figure A.1A) using the neuronal marker NeuN, the microglia marker Iba1, the astrocyte marker Gfap, and the oligodendrocyte marker myelin basic protein (MBP). Using this approach, the amygdala showed enrichment in neurons, microglia, and astrocytes. In contrast, the thalamus was enriched for oligodendrocytes, whereas the motor cortex was enriched in neurons, with intermediate levels of oligodendrocytes and astrocytes. Taken together, these data suggest that the oligodendrocytes in the thalamus are utilizing the PPP, while other cells might be more dependent on glycolysis.

3.2. mRNA, protein and enzyme activity suggest high capacity for glycolysis and the PPP in the thalamus

To begin to assess regional activity of glycolysis versus the PPP, we measured mRNA levels of key enzymes in each of these pathways from the same three brain regions. Whereas expression of hexokinase, the enzyme which catalyzes the first step of both glycolysis and the PPP, was the same in each brain region (Figure 1D), all of the enzymes of the glycolytic pathway [phosphoglucoisomerase (PGI), phosphofructokinase (PFK), and aldolase] showed slightly greater expression in the thalamus compared to the motor cortex and amygdala. G6PD, transketolase and transaldolase, components of the pentose phosphate pathway, showed even more striking differences with much higher levels of mRNA in the thalamus as compared to the motor cortex and amygdala (Figure A.1B).

Since mRNA expression does not necessarily reflect protein levels, we performed Western blot analysis of several of these enzymes. Again, hexokinase showed little variation across brain regions (Figure A.2), whereas protein levels of phosphofructokinase (PFK), the rate-limiting enzyme of glycolysis, were low in amygdala and high in thalamus and cortex, the latter occurring despite lower mRNA levels. Western blotting of G6PD, the rate-limiting enzyme of the PPP, reflected mRNA expression with higher levels in the thalamus compared to the amygdala and cortex. Interestingly, the downstream enzyme transaldolase did not follow the same pattern, showing similar levels of protein expression in the motor cortex and thalamus, with far less in the amygdala. These data suggested that regional differences in glucose metabolism could not easily be inferred from protein levels, so we additionally assessed activity of several of these enzymes. While hexokinase mRNA and protein expression were the same in all three regions, there was higher hexokinase activity in the cortex (Figure 1E). This would suggest that either glycolysis, the PPP, or both are more active in the cortex. However, when we assessed enzymatic activity of PFK and G6PD, the rate limiting enzymes of each of these pathways, the cortex was the least active in both cases. Similar to our mRNA findings, the thalamus showed the highest activity for both PFK and G6PD.

As substrate availability is one potential driver of metabolic flux, we assessed the gene expression rates of glucose transporters in these brain regions. This analysis revealed minimal mRNA expression of insulin-dependent Slc2a2 (GLUT2) and Slc2a4 (GLUT4) transporters in the regions measured, but high transcript levels for insulin-independent Slc2a1 (GLUT1) and Slc2a3 (GLUT3) in the thalamus compared to the other two regions (Figure 1F), suggesting that increased influx of glucose could be contributing to higher activity of G6PD and PFK in this region. Differences in glucose transporters do not, however, seem to explain why G6PD activity is nearly 2-fold higher in the thalamus than the motor cortex and amygdala, whereas PFK activity is only increased by 20–40%. Instead, these may reflect differences in cell type distribution by region.

3.3. Imaging mass spectrometry demonstrates differences in products of glucose metabolism in different brain regions

To more directly evaluate regional differences in glucose metabolism across the brain, we employed MALDI imaging mass spectrometry (IMS) [13]. Using this technique, mouse brain sections were analyzed at 100 μm resolution via Fourier transform-ion cyclotron resonance mass spectrometry (FT-ICR MS) in the negative ion mode. Many metabolites in the glucose metabolic pathway were detected at high enough abundance to be reliably detected across the brain (Table A.2). The distribution of each metabolite is plotted as an ion intensity map over the entire mouse brain section (hereafter referred to as the metabolite ion map). Unique regional patterns of distribution for hexose phosphate and hexose bisphosphate were determined (Figure 2A). Using MS^3 on a linear ion trap, the primary hexose bisphosphate measured in the sections was identified as the glycolytic intermediate fructose-1,6-bisphosphate (Figure 2B). An overlay was made of the metabolite ion maps and the brain atlas map [14], highlighting the distinct regional distribution of hexose phosphate and hexose bisphosphate (Figure 2C). Nissl stain of serial sections was used to confirm landmarks and determine the most appropriate brain atlas map for overlay. By overlaying a brain atlas map on the metabolite ion maps we were able to identify even smaller structures such as the mammillothalamic tracts. These data were then quantitated in the three key regions analyzed above (Figure 2D), as well as eight additional regions of interest (Figure 2E).

Across brain regions there were only modest (<50%) variations in the levels of hexose phosphate (Figure 2D,E). Because hexose phosphate is common to both glycolysis and the PPP, it serves as a measure of

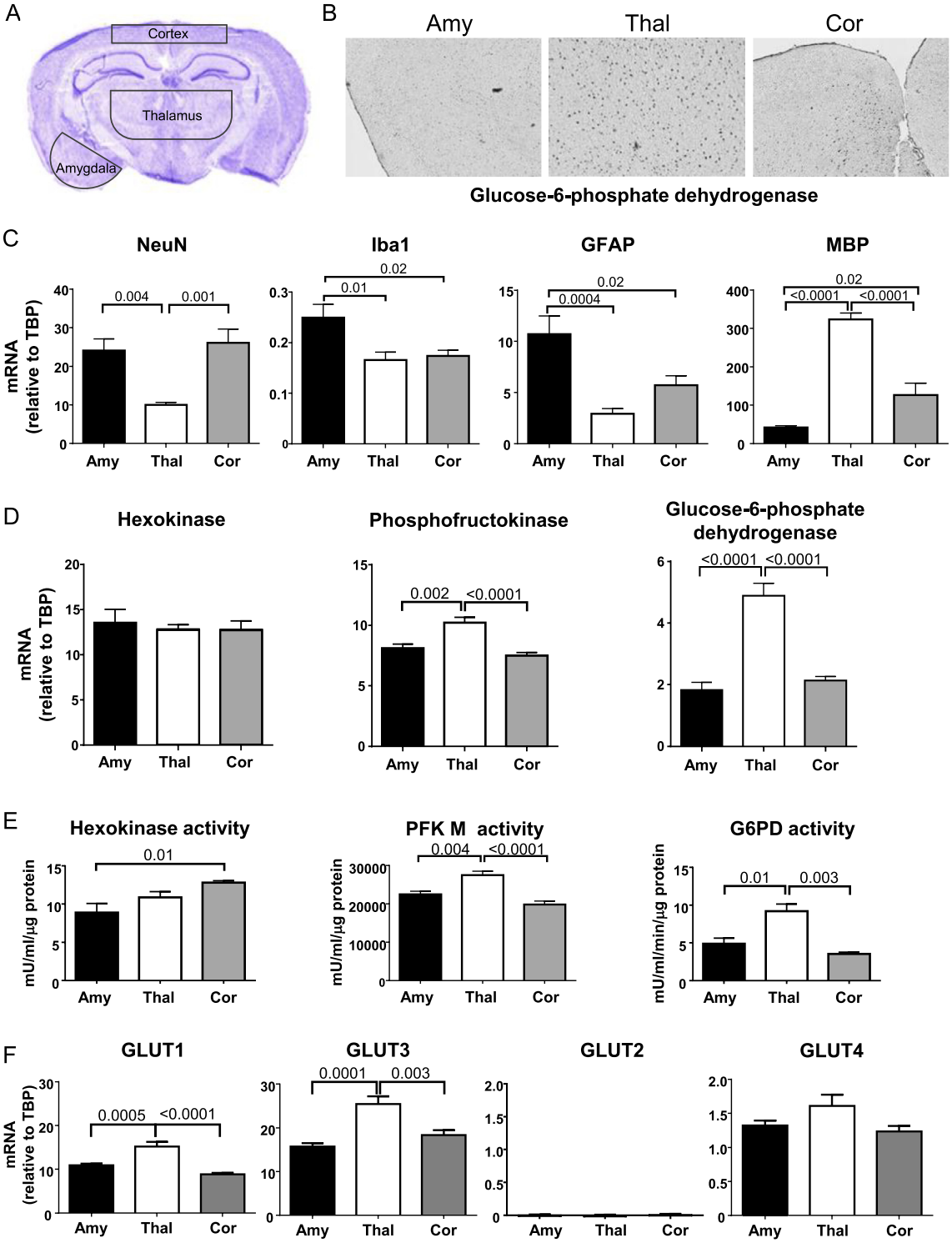

Figure 1: Differences in glucose metabolism between cortex and amygdala are not apparent despite different distributions of cells types between these regions. (A) Regions dissected for analysis are indicated by black outlines. (B) Immunohistochemistry for glucose-6-phosphate dehydrogenase across brain regions. (C) mRNA taken from amygdala (Amy), thalamus (Thal) and motor cortex (Cor) were compared by qPCR for expression of markers of neurons (NeuN), microglia (Iba1), astrocytes (GFAP) and oligodendrocytes (MBP), as well as (D) expression of enzymes involved in glycolysis and the PPP. N = 8. (E) Hexokinase activity N = 6, Glucose-6-phosphate dehydrogenase (G6PD) activity N = 3, and Phosphofructokinase type M (PFK M) activity N = 6 were performed on separate cohorts of mice. (F) Expression of glucose transporters across brain regions as measured by qPCR. N = 8.

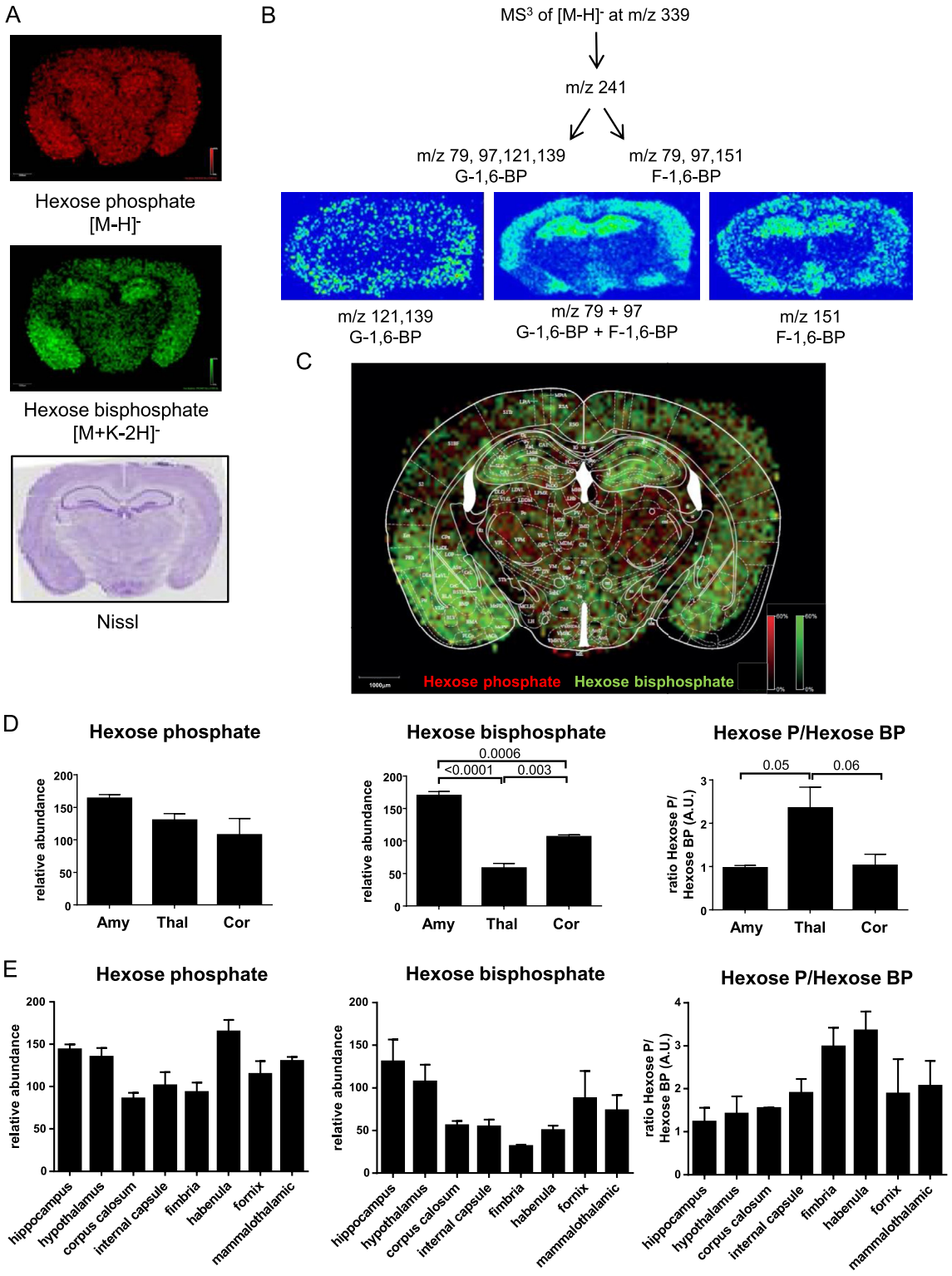

Figure 2: Glycolytic intermediate hexose bisphosphate differs by brain region. Using imaging mass spectrometry (IMS) at 100 μm resolution, (A) the distributions of hexose phosphate (top) and hexose bisphosphate (middle) were determined in coronal brain sections. Nissl stain was performed on a serial brain section (bottom). (B) To determine the identity of the hexose bisphosphate MS^3 was performed, demonstrating that the majority of the hexose bisphosphate measured was the glycolytic intermediate fructose-1,6-bisphosphate. N = 4. (C) Overlay image of hexose monophosphate and hexose bisphosphate with brain region map showing identifiable brain regions on IMS. (D) Relative abundance of hexose phosphate, hexose bisphosphate and a ratio of the two for amygdala, thalamus, and cortex and (E) 8 additional brain regions. N = 3.

regional glucose uptake. By contrast, hexose bisphosphate (i.e., fructose-1,6-bisphosphate), which is exclusive to glycolysis, varied by more than 4-fold, demonstrating the wide regional variation in the use of glucose for glycolysis versus the PPP. While direct quantitative comparisons of hexose phosphate (HP) and hexose bisphosphate (HBP) are not possible because of differences in ionization efficiency between metabolites, the ratio of HP/HBP can serve as an index of glucose entering a region of brain to glucose proceeding through the glycolytic pathway. Thus, this ratio can be compared across brain regions. Using this approach, it is clear that the highest ratio of HP to HBP was in the thalamus (Figure 2D, right panel). This also suggests that the higher hexose bisphosphate in the amygdala was a result of increased glucose delivery to the region, but that the amygdala and cortex are similarly dependent on glycolysis (Figure 2D, right panel), though differences in ion suppression based on brain region cannot be ruled out. These data support the hypothesis that in comparison to the amygdala and motor cortex, more of the glucose utilized by the thalamus is going into the PPP.

3.4. ATP is high in glycolytic regions and white matter tracts where glycolysis and PPP are low

Glycolysis is the major mechanism for cellular ATP production by providing substrate for oxidative phosphorylation. In contrast, the PPP is largely responsible for generating NADPH. From the same brain sections used in Figure 2, metabolite ion maps for relative abundance of ATP and ADP were constructed (Figure 3A). In contrast to ATP, which varied in abundance by up to 250-fold across brain regions, ADP differed by less than 1.3-fold. When overlaid with brain regional

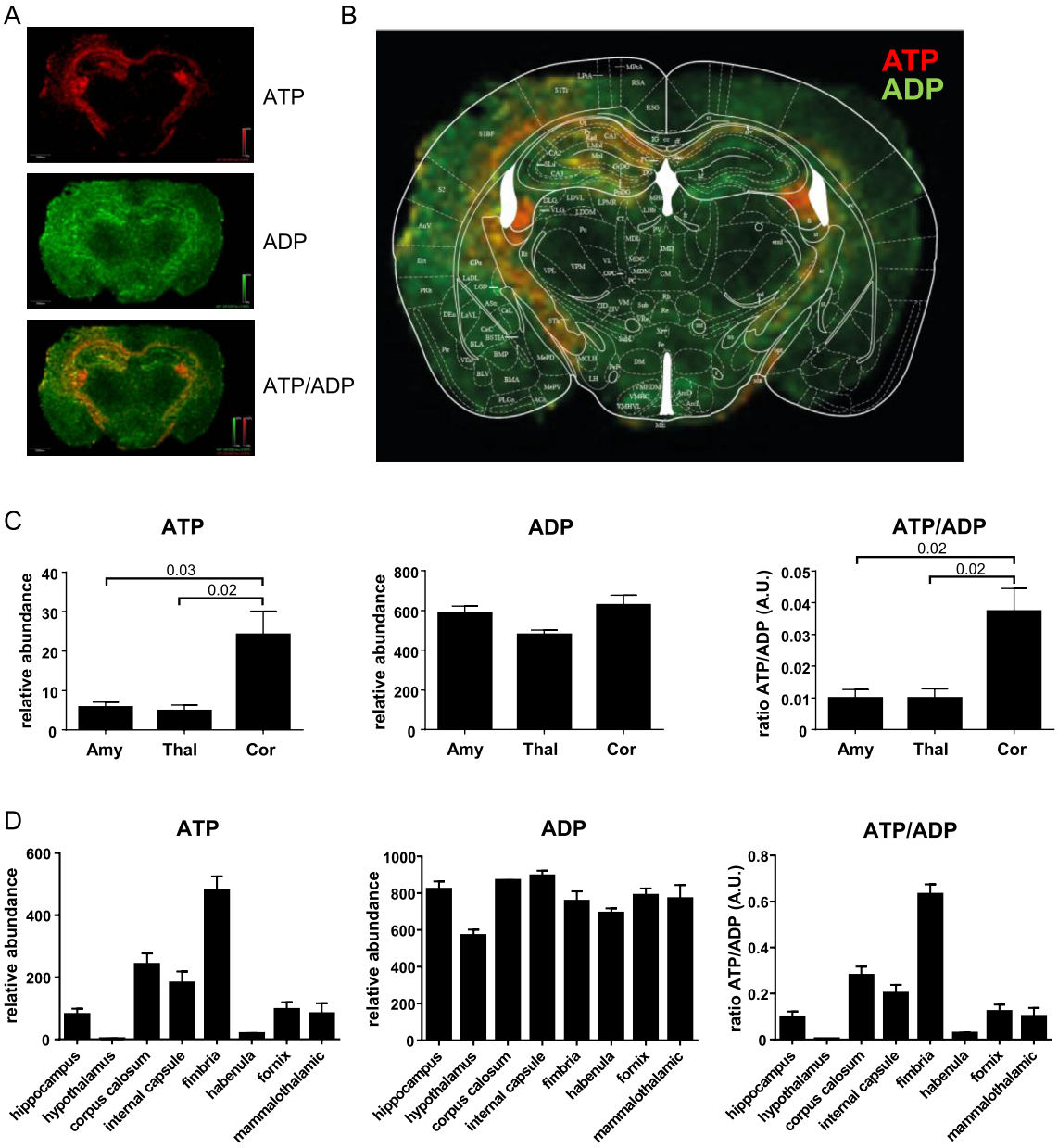

Figure 3: ATP levels vary dramatically across the brain. (A) IMS images of ATP (top), ADP (middle), and the two overlaid (bottom) from the same brains used in Figure 2. (B) Brain map overlaying IMS images highlights much higher ATP in white matter tracts and low ATP in the amygdala and thalamus. (C) Relative abundance of ATP, ADP, and the ratio of the two for amygdala, thalamus, and cortex and (D) 8 additional brain regions. N = 3.

structure (Figure 3B), it was clear that many regions of high ATP/ADP ratio corresponded to regions of low hexose phosphate/hexose bisphosphate, such as the hippocampus, but also white matter tracts such as the internal capsule and fimbria. Imaging mass spectrometry showed high ATP/ADP ratios in the motor cortex and lower levels in the thalamus, reflecting the predicted difference in glycolysis versus the PPP in these regions (Figure 3C). Interestingly, the amygdala presented a more complex picture, with low hexose phosphate/hexose bisphosphate but low ATP/ADP ratios, suggesting that there is either very high utilization of ATP in this region or that the products of glycolysis are not being used for oxidative phosphorylation. However, these differences were modest compared to the myelinated structures, such as the corpus callosum, internal capsule, and fimbria which showed very high ATP/ADP (Figure 3D). It is worth noting that these three areas, which are rich in highly myelinated axons with relatively few cell bodies, did not have low hexose phosphate/hexose bisphosphate (Figures 2E and 3D), suggesting ATP production through alternative pathways, such as the lactate shuttle from oligodendrocytes [15].

3.5. Regional distribution of hexose bisphosphate and ATP are not changed with fasting but lactate distribution is dramatically impacted

To determine how regional brain metabolism might change during a physiological stress, we compared ad libitum fed mice with mice subjected to an overnight fast. For hexose phosphate and bisphosphate, ATP, and ADP, the patterns of regional differences were similar in both the fed and fasted state, indicating the ability of brain metabolism to maintain homeostasis (Figure 4A). In contrast, tissue levels of lactate showed a significant increase in the fasted state in both the cortex and hippocampus, with no change in the thalamus, hypothalamus, or amygdala (Figure 4B). This is consistent with previous studies of whole brain demonstrating increased lactate in the fasted state [16], but to our knowledge, this is the first demonstration that this increase in lactate is regional, occurring mostly in the cortex and hippocampus.

4. DISCUSSION

Understanding of brain metabolism is key to understanding many disorders affecting the brain, including both primary brain disorders, like major mental illness and Alzheimer's disease and metabolically driven diseases such as diabetes [17,18]. In contrast to other tissues which are relatively homogenous in cell type, this challenge is compounded by the fact that the brain has distinct regional anatomy, where each region is activated by different stimuli, and made up of multiple cell types, which differ in their function and metabolism.

To this end, we employed a combination of methods to define the fate of glucose metabolites in the brain with high spatial resolution and in a nutrition-dependent manner. We investigated many steps across these pathways (Figure 4C). We show that while conventional molecular biology methods may give a snapshot of mRNA, protein, and enzyme activities, these methods often provide quantitatively conflicting information. Using imaging mass spectrometry to perform untargeted metabolite analysis across entire brain sections it is possible to determine metabolites specific for a pathway and a more direct measure of pathway activation [19]. Indeed, using IMS we were able to simultaneously measure metabolites representing the input to both glycolysis and the PPP, hexose phosphate, an intermediate in glycolysis, hexose bisphosphate, and the end-product of glycolysis/oxidative phosphorylation, ATP, across whole brain sections at 100 μm resolution. This provides a more complete picture of brain glucose metabolism with high resolution.

IMS has emerged as a powerful tool for the measurement of brain lipid levels. The brain exhibits huge variability and specificity in lipid composition [20]. IMS has revealed novel long-term alterations in regional brain lipid distribution in neurodegenerative diseases [21,22]. However, since the brain does not use lipids as a major fuel source, changes in lipid composition reflect long-term changes, in contrast to the acute alterations seen with glucose metabolism [23,24]. In this study, we have extended the utility of IMS further, for the interrogation of the much more dynamic glucose metabolic pathway.

As with other untargeted metabolomic platforms, with imaging mass spectrometry, there were many peaks found whose identity is unknown and others which were expected, but not detected due to technical limitations. As both the IMS and metabolomics fields continue to develop, the ability to detect and identify even more metabolites will also grow. This will only enhance the ability to interrogate complex metabolic pathways. Another limitation of imaging mass spectrometry is that all measurements come from a single point in time, and as such, IMS does not measure flux. However, the simultaneous assessment of multiple metabolites in a pathway does produce a metabolic picture that reflects flux through the system and does so across different regions of the brain.

The data of the present study show that activity of phosphofructokinase, often referred to as the rate-limiting step of glycolysis, does not accurately reflect metabolite levels in areas where the PPP is quite active, such as the thalamus. This has also been found to be true in colon cancer cells, where GAPDH was determined to be the rate-limiting step in glycolysis and fructose-1,6-bisphosphate the most accurate metabolite for measuring flux through the glycolytic pathway [25]. In addition, IMS can be used to assess the impact of physiological or pathophysiological changes to a metabolic pathway, as illustrated by the data showing regional changes in lactate abundance during fasting. Interestingly, this occurs while the quantity and distribution of other metabolites, such as ATP, is preserved, indicating the importance of metabolic flexibility to ensure constant ATP levels for proper brain physiology [26]. While there are other neuroimaging techniques, which can be used to analyze brain metabolism in living subjects, such as magnetic resonance imaging (MRI) or positron emission tomography (PET), these are able to detect far fewer metabolites than with IMS. Also, the resolution of these techniques (about 150–500 μm) is significantly less than the 10–100 μm currently achievable with IMS. In addition, PET imaging, which is commonly used to examine glucose uptake in the brain, gives no information on how the glucose is metabolized or of other metabolites present. Thus, in most cases, IMS and neuroimaging do not address the same questions, underlining the different scientific values of each technique.

Precise control of neuronal glucose metabolism via the glycolytic and PPP is important for neuronal function, activation, and neuronal survival [27,28]. Brain glucose metabolism changes with aging, with aerobic glycolysis decreasing in a region specific manner in aged humans [27]. IMS can be used in the future to better understand the effects of aging on regional brain metabolism. Alterations in metabolites in the aging brain caused by diet may reveal new connections between obesity and dementia. As glucose metabolites can regulate multiple signaling pathways, from basal metabolism up to survival pathways such as autophagy and mitochondrial-induced apoptosis, use of IMS will improve our ability to identify potentially unexpected regional changes in brain glucose metabolism as well as identify novel pathways in brain areas prone to neurodegeneration.

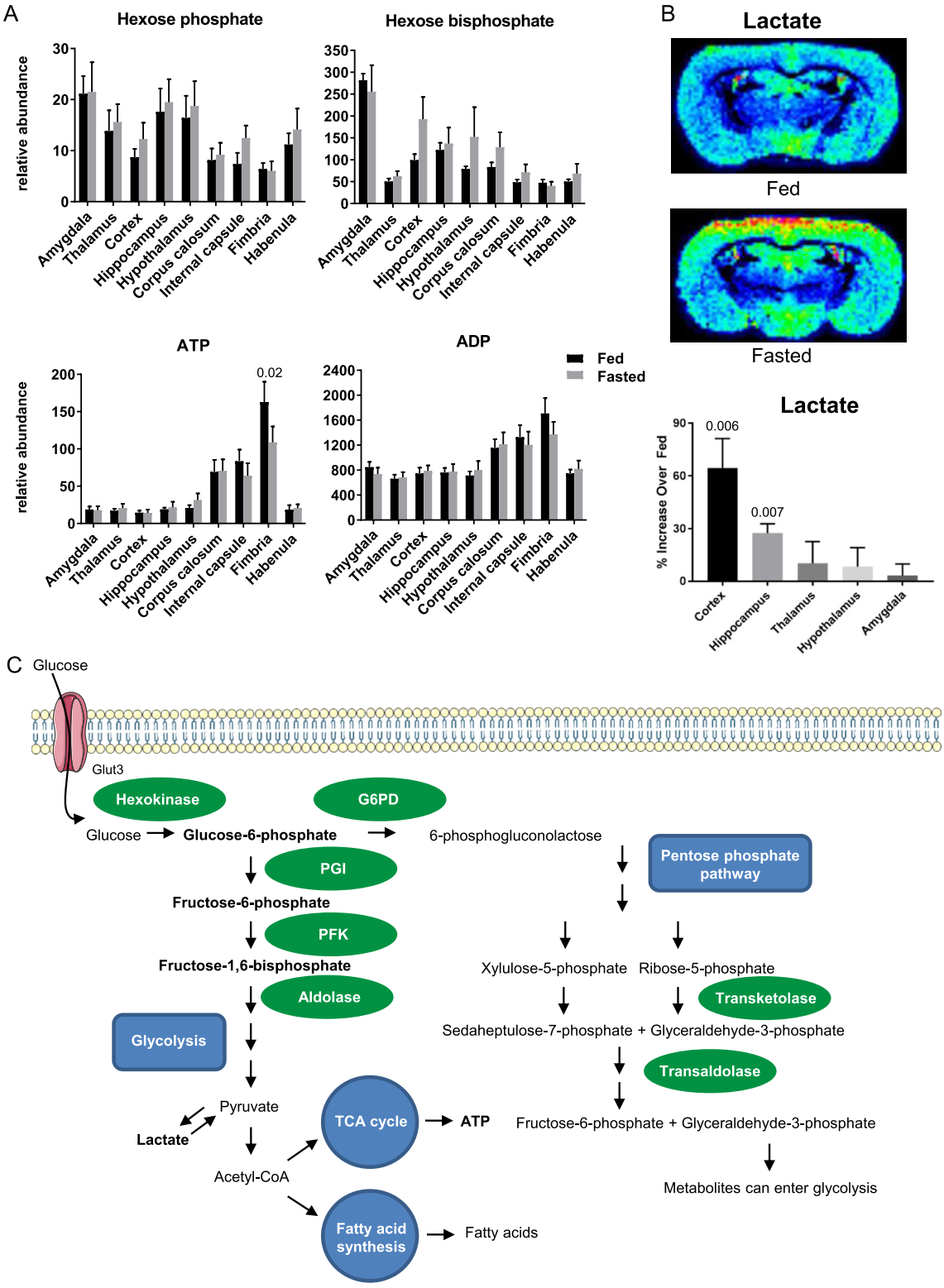

Figure 4: Fasting causes regional increases in brain lactate. (A) Fasting did not induce changes in hexose phosphate, hexose bisphosphate, ATP, or ADP compared to random fed mice. (B) Fasting induced increases in lactate in the cortex and hippocampus without changing levels in other brain regions. N = 5. (C) After glucose enters a cell it can be metabolized through glycolysis (left) or the pentose phosphate pathway (right). Enzymes assessed are in green ovals. Metabolites measured are in bold. G6PD = glucose-6-phosphate dehydrogenase, PGI = phosphoglucoisomerase, PFK = phosphofructokinase.

FUNDING

This work was supported by R01 DK033201, R01 DK031036, and the Mary K. Iacocca Professorship (to C.R.K.), P30 DK036836 (Joslin DERC Core Facilities), 5P41 GM103391-07 (to R.M.C.), and DFG project KL2399-4/1 (A K.). The work of A.K. was also supported by the Federal Ministry of Education and Research (German Center for Diabetes Research, Grant No. 01GI092). The funding sources had no role in the design, collection, or publication of this data.

CONFLICT OF INTEREST

The authors declare no competing financial interests.

APPENDIX A. SUPPLEMENTARY DATA

Supplementary data related to this article can be found at https://doi.org/10.1016/j.molmet.2018.03.013.

REFERENCES

[1] Ferris, H.A., Perry, R.J., Moreira, G.V., Shulman, G.I., Horton, J.D., Kahn, C.R., 2017. Loss of astrocyte cholesterol synthesis disrupts neuronal function and alters whole-body metabolism. Proc Natl Acad Sci U S A 114(5):1189–1194.

[2] Jais, A., Solas, M., Backes, H., Chaurasia, B., Kleinridders, A., Theurich, S., et al., 2016. Myeloid-cell-Derived VEGF maintains brain glucose uptake and limits cognitive impairment in obesity. Cell 165(4):882–895.

[3] Raichle, M.E., Gusnard, D.A., 2002. Appraising the brain's energy budget. Proc Natl Acad Sci U S A 99(16):10237–10239.

[4] McCrimmon, R.J., Ryan, C.M., Frier, B.M., 2012. Diabetes and cognitive dysfunction. Lancet 379(9833):2291–2299.

[5] Hayes, J.D., McLellan, L.I., 1999. Glutathione and glutathione-dependent enzymes represent a co-ordinately regulated defence against oxidative stress. Free Radical Research 31(4):273–300.

[6] Belanger, M., Allaman, I., Magistretti, P.J., 2011. Brain energy metabolism: focus on astrocyte-neuron metabolic cooperation. Cell Metabolism 14(6):724–738.

[7] Howarth, C., Gleeson, P., Attwell, D., 2012. Updated energy budgets for neural computation in the neocortex and cerebellum. Journal of Cerebral Blood Flow and Metabolism 32(7):1222–1232.

[8] Herculano-Houzel, S., Mota, B., Lent, R., 2006. Cellular scaling rules for rodent brains. Proc Natl Acad Sci U S A 103(32):12138–12143.

[9] Sanchez-Abarca, L.I., Tabernero, A., Medina, J.M., 2001. Oligodendrocytes use lactate as a source of energy and as a precursor of lipids. Glia 36(3):321–329.

[10] Amaral, A.I., Hadera, M.G., Tavares, J.M., Kotter, M.R., Sonnewald, U., 2016. Characterization of glucose-related metabolic pathways in differentiated rat oligodendrocyte lineage cells. Glia 64(1):21–34.

[11] Bouzier-Sore, A.K., Bolanos, J.P., 2015. Uncertainties in pentose-phosphate pathway flux assessment underestimate its contribution to neuronal glucose consumption: relevance for neurodegeneration and aging. Frontiers in Aging Neuroscience 7:89.

[12] Tian, W.N., Pignatare, J.N., Stanton, R.C., 1994. Signal transduction proteins that associate with the platelet-derived growth factor (PDGF) receptor mediate the PDGF-induced release of glucose-6-phosphate dehydrogenase from permeabilized cells. Journal of Biological Chemistry 269(20):14798–14805.

[13] Norris, J.L., Caprioli, R.M., 2013. Analysis of tissue specimens by matrix-assisted laser desorption/ionization imaging mass spectrometry in biological and clinical research. Chemical Reviews 113(4):2309–2342.

[14] Franklin, K.B.J., Paxinos, G., 2008. The mouse brain in stereotaxic coordinates, 3rd ed. Amsterdam: Boston: Elsevier/Academic Press.

[15] Funfschilling, U., Supplie, L.M., Mahad, D., Boretius, S., Saab, A.S., Edgar, J., et al., 2012. Glycolytic oligodendrocytes maintain myelin and long-term axonal integrity. Nature 485(7399):517–521.

[16] Pan, J.W., Rothman, T.L., Behar, K.L., Stein, D.T., Hetherington, H.P., 2000. Human brain beta-hydroxybutyrate and lactate increase in fasting-induced ketosis. Journal of Cerebral Blood Flow and Metabolism 20(10):1502–1507.

[17] Dean, B., Thomas, N., Scarr, E., Udawela, M., 2016. Evidence for impaired glucose metabolism in the striatum, obtained postmortem, from some subjects with schizophrenia. Translational Psychiatry 6(11):e949.

[18] Teune, L.K., Bartels, A.L., de Jong, B.M., Willemsen, A.T., Eshuis, S.A., de Vries, J.J., et al., 2010. Typical cerebral metabolic patterns in neurodegenerative brain diseases. Movement Disorders 25(14):2395–2404.

[19] Gieger, C., Geistlinger, L., Altmaier, E., Hrabe de Angelis, M., Kronenberg, F., Meitinger, T., et al., 2008. Genetics meets metabolomics: a genome-wide association study of metabolite profiles in human serum. PLoS Genetics 4(11):e1000282.

[20] Veloso, A., Fernandez, R., Astigarraga, E., Barreda-Gomez, G., Manuel, I., Giralt, M.T., et al., 2011. Distribution of lipids in human brain. Analytical and Bioanalytical Chemistry 401(1):89–101.

[21] Mendis, L.H., Grey, A.C., Faull, R.L., Curtis, M.A., 2016. Hippocampal lipid differences in Alzheimer's disease: a human brain study using matrix-assisted laser desorption/ionization-imaging mass spectrometry. Brain and Behavior 6(10):e00517.

[22] Gonzalez de San Roman, E., Manuel, I., Giralt, M.T., Ferrer, I., Rodriguez-Puertas, R., 2017. Imaging mass spectrometry (IMS) of cortical lipids from preclinical to severe stages of Alzheimer's disease. Biochimica et Biophysica Acta 1859(9 Pt B):1604–1614.

[23] Ando, S., Tanaka, Y., Toyoda, Y., Kon, K., 2003. Turnover of myelin lipids in aging brain. Neurochemical Research 28(1):5–13.

[24] Hayes, L.W., Jungalwala, F.B., 1976. Synthesis and turnover of cerebrosides and phosphatidylserine of myelin and microsomal fractions of adult and developing rat brain. Biochemical Journal 160(2):195–204.

[25] Shestov, A.A., Liu, X., Ser, Z., Cluntun, A.A., Hung, Y.P., Huang, L., et al., 2014. Quantitative determinants of aerobic glycolysis identify flux through the enzyme GAPDH as a limiting step. Elife 3.

[26] Camandola, S., Mattson, M.P., 2017. Brain metabolism in health, aging, and neurodegeneration. The EMBO Journal 36(11):1474–1492.

[27] Vaughn, A.E., Deshmukh, M., 2008. Glucose metabolism inhibits apoptosis in neurons and cancer cells by redox inactivation of cytochrome c. Nature Cell Biology 10(12):1477–1483.

[28] Diaz-Garcia, C.M., Mongeon, R., Lahmann, C., Koveal, D., Zucker, H., Yellen, G., 2017. Neuronal stimulation triggers neuronal glycolysis and not lactate uptake. Cell Metabolism 26(2), 361–374 e4.

